Journal of Geoscience and Environment Protection, 2025, 13(3), 29-46
https://www.scirp.org/journal/gep
ISSN Online: 2327-4344
ISSN Print: 2327-4336

Interannual Relationship between ENSO and Tropical Cyclone Genesis over the Southwest Indian Ocean and Its Modulation by the Interdecadal Pacific Oscillation

Daniel Stephano Semgomba[1,2*], Jiechun Deng[1], Philemon Henry King'uza[1,2]

[1]School of Atmospheric Sciences, Nanjing University of Information Science & Technology, Nanjing, China
[2]Tanzania Meteorological Authority, Dodoma, Tanzania
Email: *semgomba@gmail.com

How to cite this paper: Semgomba, D. S., Deng, J. C., & King'uza, P. H. (2025). Interannual Relationship between ENSO and Tropical Cyclone Genesis over the Southwest Indian Ocean and Its Modulation by the Interdecadal Pacific Oscillation. *Journal of Geoscience and Environment Protection, 13,* 29-46.
https://doi.org/10.4236/gep.2025.133002

Received: February 7, 2025
Accepted: March 10, 2025
Published: March 13, 2025

Abstract

This study investigates the interannual relationship between El Niño-Southern Oscillation (ENSO) and tropical cyclone (TC) genesis potential (measured by the Dynamic Genesis Potential Index or DGPI) over the Southwest Indian Ocean (SWIO) and its modulation by the Interdecadal Pacific Oscillation (IPO) during 1959-2020 based on observation and reanalysis. Results show that DGPI can well capture the spatial distribution and seasonal cycle of TC genesis over the SWIO. A positive correlation is found between ENSO and the SWIO-DGPI on interannual timescales, with higher (lower) DGPI and increased (decreased) TC occurrence frequency during El Niño (La Niña) years, indicating an important role of ENSO in modulating TC activity in the SWIO. Further analyses show that ENSO favors the SWIO TC genesis primarily through modulating vertical wind shear and upward motion. Furthermore, the interannual relationship between ENSO and the SWIO DGPI also exhibits remarkable interdecadal variations that are likely modulated by the IPO with strong (weak) correlation in positive (negative) IPO phases. This is because the ENSO-driven anomalies of vertical wind shear, upward motion, and low-level vorticity are larger under positive IPO phases than its negative phases, which favor the sensitivity of the SWIO TC genesis to ENSO and thus promote a higher correlation between the two. These findings highlight the importance of considering interdecadal variability when assessing the ENSO-TC relationship over the SWIO and contribute to improving seasonal prediction of TCs in the region.

Keywords

Dynamic Genesis Potential Index (DGPI), Tropical Cyclogenesis, Southwest

Indian Ocean (SWIO), El Niño-Southern Oscillation (ENSO), Interdecadal Pacific Oscillation (IPO)

1. Introduction

Tropical cyclones (TCs) are considered the most destructive natural hazards within seven basins, with a mean of 86 TCs every year (Wang & Murakami, 2020). Particularly, in the Southwest Indian Ocean (SWIO), around 9 to 11 TCs occur every season from November to April (Muthige et al., 2018), significantly impacting lives, properties, and infrastructures. Thus, understanding the controls on the formation of the SWIO TCs is very important for improving predictive models and preparedness strategies in the region.

The climatology of tropical cyclone activity in the global oceans is commonly explained by the genesis potential indices (GPIs) from several large-scale environmental parameters (Camargo & Wing, 2016). They have been widely utilized to understand observed mean state climatology of tropical cyclogenesis (Camargo et al., 2007) and climatological variability induced by modes of climate variability on seasonal timescales (Camargo et al., 2007; Gray, 1979). The dynamic and thermodynamic components of most GPIs can capture the known physics required for the development and maintenance of a tropical cyclone (Murakami & Wang, 2022). The dynamic component represents background rotation, which is commonly defined by the lower-tropospheric (e.g., 850 hPa) absolute vorticity. The maximum potential intensity commonly represents the energetic potential of the atmosphere to support a tropical cyclone, which is the thermodynamic component of GPI (Bister & Emanuel, 2002). Additionally, the mid-tropospheric vertical velocity is also a factor that measures seed activity (Hsieh et al., 2023). In the Southern Hemisphere, Camargo et al. (2007) have further identified vertical wind shear and mid-tropospheric relative humidity as the key factors influencing tropical cyclone activity.

It is suggested that El Niño-Southern Oscillation (ENSO) may play a role in regulating the TC genesis and frequency over different oceanic basins, including the SWIO. ENSO is among the large-scale interactions of the atmosphere with the ocean that influence global atmospheric circulation. Many researchers have examined the effects of ENSO on tropical storm activity in oceanic basins. For example, the TC genesis frequency tends to increase over the southeastern part of the western North Pacific but decreases over the northwestern part during the development of the El Niño phase (Wang & Chan, 2002). In the Atlantic Ocean, there are fewer TCs during El Niño years, while the opposite occurs in La Niña years (Camargo et al., 2007). In particular, the TC genesis increased in the western of 75˚E and decreased to the east, compared to La Nina years, over the SWIO during El Nino years (Ho et al., 2006). Kuleshov et al. (2009) suggested that the TC genesis decreased in the western South Indian Ocean but increased in the east,

and they found that sharp wind-shear gradients in tropical cyclone regions introduce some complexity to the analysis of ENSO's impact on tropical cyclone activity.

On the other hand, the TC genesis can also be modulated by climate variability at lower frequencies. Pacific Decadal Variability (PDV) refers to a long-term variation in SST and atmospheric patterns in the Pacific Ocean, typically over decades. Pacific Decadal Oscillation (PDO) is a part of PDV with alternating warm and cold phases that last 20 - 30 years. The warm phase has heightened SSTs in the eastern and central Pacific, which impacts atmospheric circulation. The Interdecadal Pacific Oscillation (IPO) has a longer time scale than the PDO and incorporates more variability in the entire Pacific Ocean, including the tropics and Southern Hemisphere (Lorenzo et al., 2025). The Atlantic Multidecadal Oscillation (AMO) refers to the multidecadal variability in the Atlantic Ocean, characterized by slow changes in SST for approximately 60 - 80 years (Moore et al., 2017). PDV, particularly including PDO or the associated IPO, and the AMO have been implicated in periods of acceleration and slowdown in the rate of global warming at the surface in the post-industrial period (Crowley et al., 2014; England et al., 2014; Fyfe et al., 2016; Kosaka & Xie, 2013, 2016; Maher et al., 2014). These patterns are also responsible for coherent and persistent hydroclimatic impacts globally (Henley, 2017). For example, during the positive IPO phase, TC genesis tends to increase over the Northern Atlantic and reduce over the eastern North Atlantic, likely due to the changes in vertical wind shear and thus genesis potential (Li et al., 2015). On the other hand, these low-frequency oscillations (e.g., IPO and PDO) also play a key role in modulating ENSO activities and thus their associated teleconnections (Gershunov & Barnett, 1998; Livezey & Smith, 1999), which should further affect the ENSO's impacts on remote climates, such as Australian precipitation (Power et al., 1999). However, it remains unclear whether and how the IPO can modulate the interannual relationship between ENSO and TC genesis over different oceanic basins, particularly the SWIO.

In this study, we intend to explore the interannual relationship between ENSO and TC genesis (as measured by a dynamical GPI or DGPI shown below) over the SWIO, with a special focus on its modulation by the IPO. The study seeks to examine the mechanisms underlying the ENSO-DGPI relationship over the SWIO and the significant role of the IPO in modulating this interannual relationship. The remainder of the paper is organized as follows. Section 2 describes the data and methodology. The climatology of DGPI over SWIO is described in Section 3. Section 4 provides an analysis of the interannual relationship between ENSO and DGPI over the SWIO and the possible mechanism. Section 5 explores the modulation effect of the IPO on the interannual relation between the two. The conclusion is drawn in Section 6.

2. Data and Methodology

We used the monthly atmospheric and oceanic fields from the fifth generation of

the European Centre for Medium-range Weather Forecasts (ECMWF) reanalysis (ERA5; Hersbach et al., 2023) on a 0.25˚grid from 1959 to 2022, including horizontal wind vectors, relative vorticity, and vertical velocity at different vertical levels, and sea surface temperature (SST). We also used the TC best track data from the International Best Track Archive for Climate Stewardship (IBTrACS Version 4.0; Knapp et al., 2010). The IBTrACS dataset consists of the TC data compiled by multiple organizations, in our study we will utilize data from the RSMC La Réunion. TCs from 1980 to 2022 with tropical storm intensity (i.e. surface wind speeds of 35 kt) or above over the SWIO basin (as shown in **Figure 1(b)**) are considered in this study.

In this study, we employed a new dynamic genesis potential index (DGPI; Wang & Murakami, 2020) for the recognition of TC genesis potential in global oceans. DGPI includes an additional dynamical dependence on the meridional shear of the zonal wind specifically in the Southern Hemisphere and no explicit dependency on potential intensity or SST slightly deviates from other GPI. The skill of DGPI has been compared to measure the climatological mean distribution and the relationship between TC genesis and ENSO, which is more skilled than other GPIs in the western North Pacific Ocean, Pacific Ocean, and the South and North Indian Ocean, similar to North Atlantic Ocean, but less skillful in the eastern North Pacific Ocean for representing the year-to-year variations of basin total GPI numbers (Wang & Murakami, 2020). According to Wang and Murakami (2020) DGPI is defined as follows:

$$\mathrm{DGPI} = V_s^{-1} U_y^2 \omega^3 \zeta_a^2 e^{-12} - 1.0 \tag{1}$$

where V_s, ζ_a, ω, and U_y are vertical wind shear between 200 hPa to 850 hPa, absolute vorticity at 850 hPa, vertical velocity, and meridional gradient of zonal wind at 500 hPa, which are defined as follows:

$$V_s = 2.0 + 0.1 \times \left| ws_{200} - ws_{850} \right| \tag{2}$$

$$\omega = 5.0 - 20 \times \omega_{500} \tag{3}$$

$$\zeta_a = 5.5 + \left| \left(\zeta_{850} + f \right) \times 10^5 \right| \tag{4}$$

$$f = 1.0 + \left| \frac{f}{f_0}, f_0 \text{ is } f \text{ at } 10^\circ\mathrm{N} \right| \tag{5}$$

$$U_y = 5.5 - \frac{\partial u_{500}}{\partial y} \times 10^5 \tag{6}$$

Note that DGPI is set to zero over the grids where SST is lower than 26˚C and latitude within 5˚ around the equator.

We also used the Niño 3.4 index to measure ENSO and thus its associated anomaly composites. The Niño 3.4 index is calculated by the average SST anomaly in the region of 5˚S - 5˚N and 170˚W - 120˚W. The El Niño (La Niña) years are defined when NDJ-mean SST anomalies averaged over this region are greater (smaller) than +0.5 (−0.5)˚C, as shown in **Table 1**. Besides, the IPO index is defined as the difference between the SST anomalies averaged over the central equa-

torial Pacific and the northwest and southwest Pacific (Henley et al., 2015). Note that all the anomaly fields and the relevant indices are linearly detrended before further analysis.

Table 1. El Niño and La Niña years are defined in this study.

ENSO type	Years
El Niño	1965/1966, 1968/1969, 1972/1973, 1982/1983, 1986/1987, 1987/1988, 1991/1992, 1994/1995, 1997/1998, 2002/2003, 2006/2007, 2009/2010, 2015/2016.
La Niña	1971/1971, 1973/1974, 1975/1976, 1984/1985, 1988/1989, 1998/1999, 1999/2000, 2007/2008, 2010/2011, 2011/2012, 2020/2021.

3. DGPI Climatology over the SWIO

Figure 1(a) shows the global distribution of DGPI in the hemispheric season with strong TC activity. In the global context, all well-known tropical cyclone-prone regions show maximum DGPI, such as the western Pacific, North Atlantic, South Pacific, and Indian Ocean basins with higher DGPI and active TC development, which agrees with previous studies (Camargo et al., 2007; Wang & Murakami, 2020). Meanwhile, low DGPI regions are associated with unfavorable conditions of TC genesis; for example, the equatorial zone with a low Coriolis force. Clearly, such a distribution may be determined by the dynamic (e.g., vorticity and wind shear) and thermodynamic (e.g., SST) factors in the TC formation. In particular, the SWIO region is one of the most important basins for TC activity over the Indian Ocean. The DGPI over the SWIO shows remarkable spatial variations with the higher DGPI along 10˚S to 20˚S that extends eastward from the African coastline toward around 90˚E (**Figure 1(b)**). This spatial heterogeneity underlines the interaction of regional or global scale drivers (Duan et al., 2021), such as the warm SSTs of the Mozambique Channel (Mavume et al., 2010).

The higher DGPI over this region reflects a higher possibility of TC genesis, especially during the austral summer with favorable conditions. Accordingly, a distinct band of high TC frequency is observed between 10˚S and 20˚S, covering the Mozambique Channel and extending eastward toward the central SWIO basin (**Figure 1(c)**), which is consistent with the high DGPI in this region (**Figure 1(b)**). In addition, we also compare the annual cycle of DGPI and observed TC frequency over the SWIO (**Figure 1(d)**). It is found that DGPI and TC activity increases markedly during the austral summer months from January to March, with the most favorable conditions for cyclogenesis (Camargo et al., 2007), while both GPI and TC show a rapid decline over the SWIO region from May through September (i.e., the winter season). The correlation coefficient (r) of their seasonal cycle reaches 0.93, indicating a very good agreement between the DGPI and actual cyclone occurrences over the SWIO. These results suggest that DGPI can be used as a proxy to measure TC genesis over the SWIO and to investigate the ENSO-DGPI relationship below.

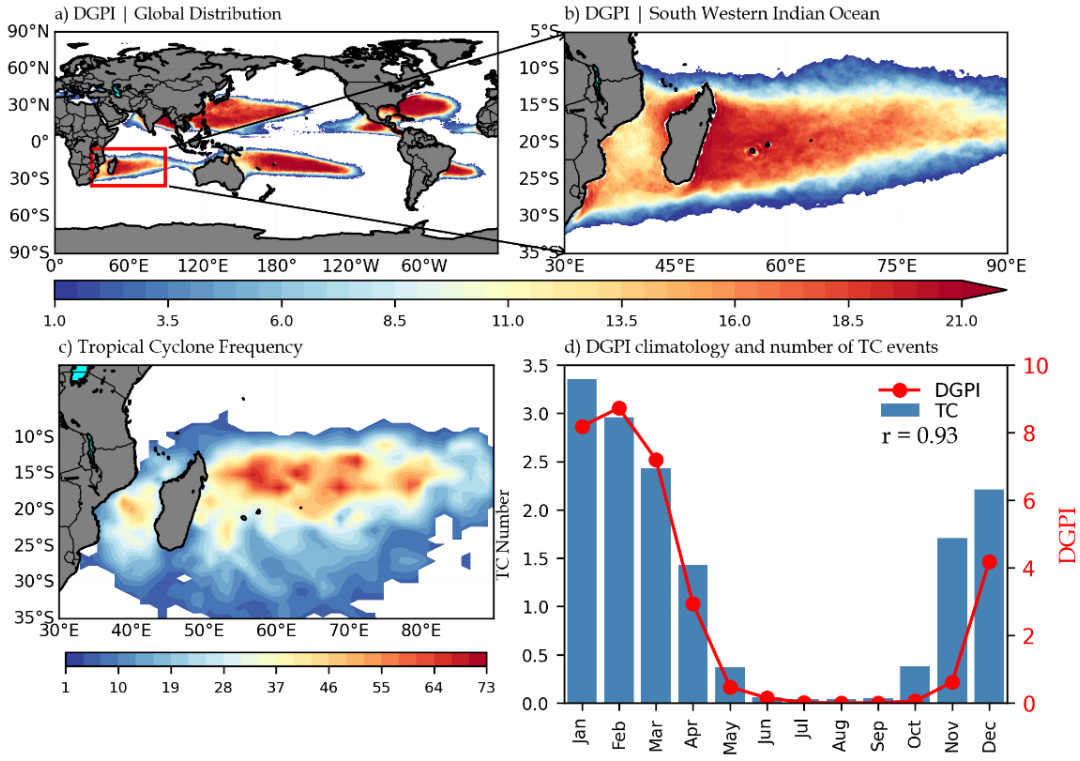

Figure 1. (a) Spatial distribution of the climatological mean DGPI (unitless) from May through October in the Northern Hemisphere and from November to April in the Southern Hemisphere; (b) Same as (a), but for the climatological mean DGPI from November to April in the Southern West Indian Ocean (SWIO); (c) Spatial distribution of observed tropical cyclone (TC) frequency (number) over the SWIO from November to April during 1980-2022 based on IBTrACS. (d) Monthly climatology of the DGPI (unitless, red line) and the TC number (number per month, blue bars) over the same region.

4. Interannual Relationship between ENSO and DGPI and the Possible Mechanism

To depict the interannual relationship between ENSO and DGPI, **Figure 2(a)** shows the spatial pattern of the correlation coefficient between the SWIO DGPI and SST anomalies over the globe. Apparently, there exists a strong positive correlation (with r above 0.5) between the SWIO DGPI and anomaly SST over the central to eastern tropical Pacific. Their close relationship indicates that ENSO may play a crucial role in the TC genesis over the SWIO during November to April when ENSO usually develops; specifically, there would be higher (lower) DGPI and thus more (less) TCs over the SWIO during the El Niño (La Niña) years. In addition, we also found a moderate positive correlation over the Indian Ocean, with the strongest correlation over the SWIO, while the DGPI is slightly anti-correlated with SST anomalies in the southeastern Indian Ocean. This relationship between DGPI and SST anomalies over the SWIO is expected as warmer local SST would favor higher DGPI and thus more TCs. As our goal is to reveal the remote relationship between ENSO and the SWIO DGPI, we also show the detrended time series of the Niño3.4 index and the SWIO DGPI in **Figure 2(b)**. Clearly, the SWIO DGPI exhibits remarkable interannual variations, which is closely corre-

lated with the Niño3.4 index (with $r = 0.5$). This further confirms that the SWIO DGPI can be remotely regulated by ENSO events.

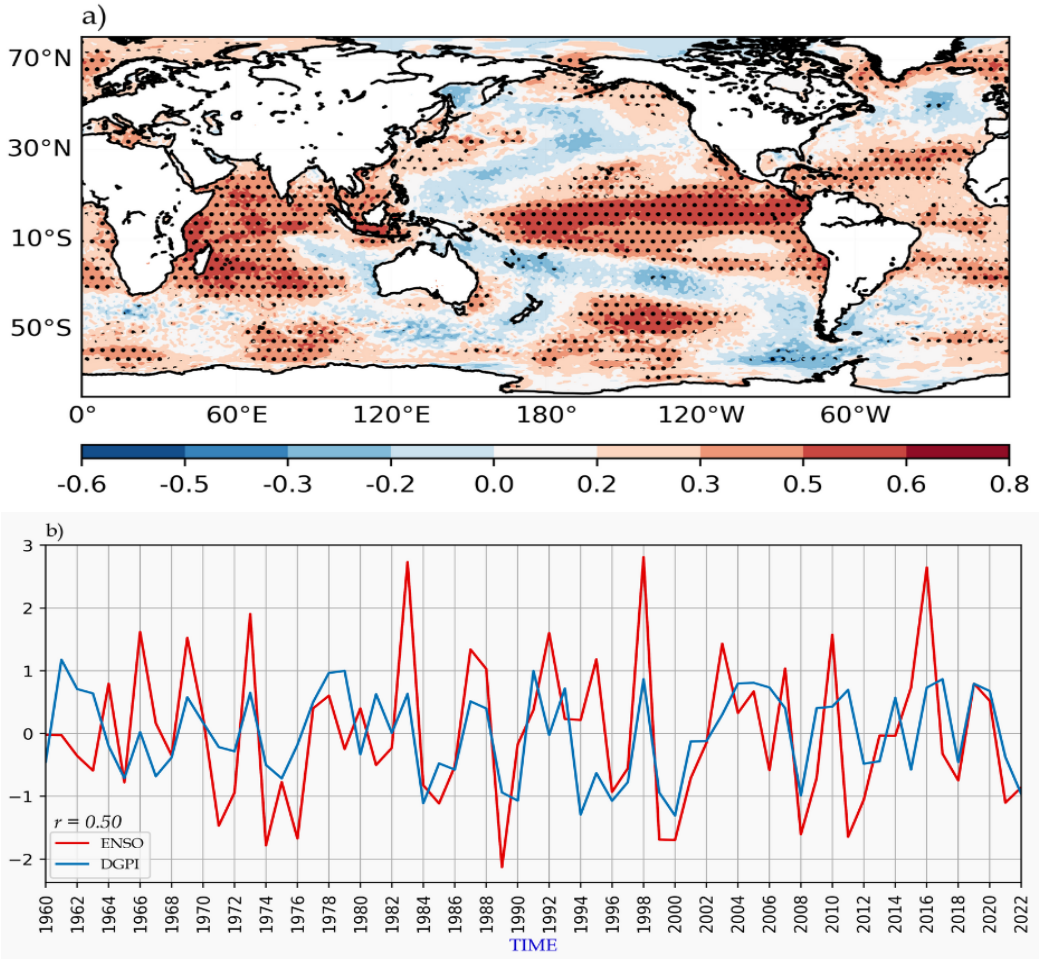

Figure 2. (a) The spatial distribution of the correlation between the SWIO DGPI and anomalous SST over the globe averaged over November to January during 1959-2022 based on ERA5 reanalysis. The stippling indicates the correlation coefficients are statistically significant at the 95% confidence level based on Student's *t-test*; (b) The detrended time series of the SWIO DGPI (unitless, blue line) and the Niño3.4 index (in ˚C, red line) averaged over November to April during 1959-2022 in ERA5.

Several studies have reported that El Niño events tend to favor TC genesis over the SWIO (e.g., Ho et al., 2006; Kuleshov et al., 2009). Thus, to further explore the relationship between ENSO and DGPI over the SWIO, **Figure 3** also shows the composite of anomalous DGPI and TC frequency over the SWIO from November to April (i.e., the period of strong TC activity there) during El Niño and La Niña events. As shown in **Figure 3(a)**, during El Niño, DGPI is significantly higher over the SWIO, suggesting the increased likelihood of TC genesis during these events. This increased DGPI agrees well with an increased frequency of tropical cyclones (**Figure 3(d)**) over the SWIO during El Niño years. In contrast, the SWIO DGPI is remarkably reduced during La Niña years (**Figure 3(b)**), together with a relatively low occurrence frequency of TCs in the region (**Figure 3(e)**). **Figure 3(c)**

and Figure 3(f) indicate contrasting spatial patterns of DGPI and TC frequency under different ENSO years. The difference patterns further show that DGPI is much higher over the SWIO during El Niño years relative to that during La Niña years (Figure 3(c)), which is consistent with the higher occurrence frequency of TCs in the SWIO (Figure 3(f)).

In summary, our analysis suggests that the DGPI over the SWIO is closely correlated with ENSO; that is, there would be a conducive environment for TC genesis over the SWIO region during El Niño years with higher occurrence frequencies of TCs under higher DGPI, while the opposite is seen during La Niña years.

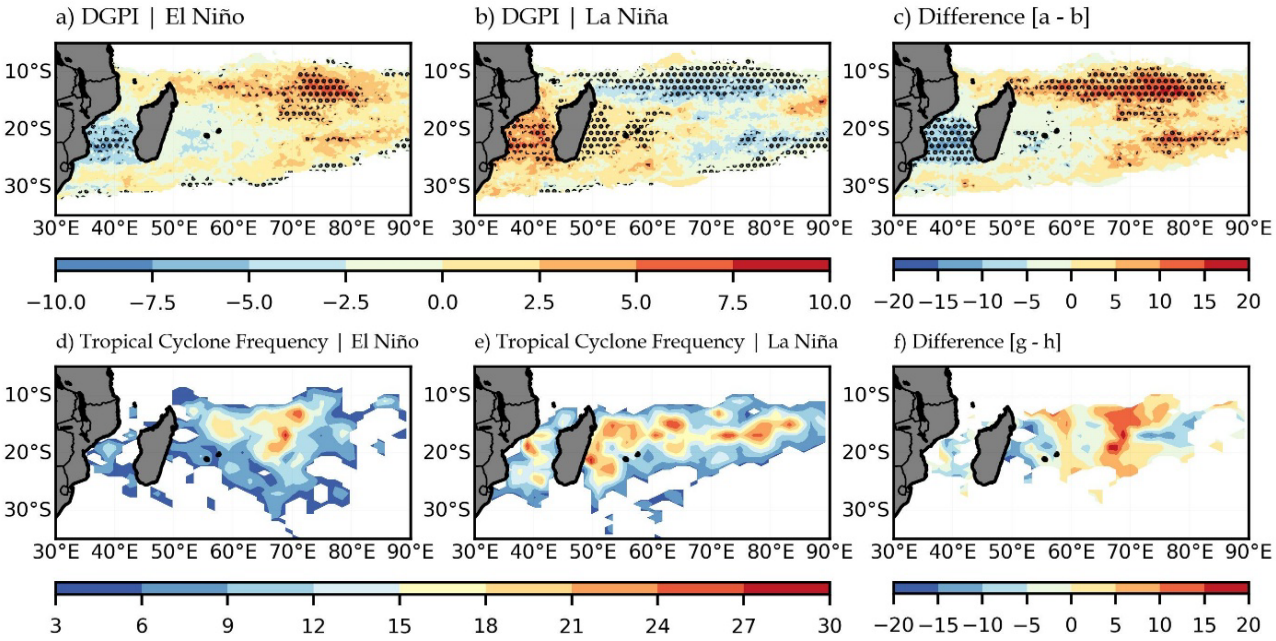

Figure 3. Spatial distribution of DGPI from November to April during (a) El Niño and (b) La Niña years and (c) their difference (i.e., El Niño years minus La Niña years) during 1959-2022 based on ERA5. (d)-(f) Same as (a)-(c), but for TC frequency based on IBTrACS. The stippling indicates the difference is statistically significant at the 95% confidence level.

To further investigate how ENSO can modulate the TC genesis potential over the SWIO, Figure 4 shows the differences of several controlling factors related to TC genesis potential (referring to the DGPI definition in Section 2) between El Niño and La Niña years, including vertical wind shear, low-level vorticity, the meridional gradient of zonal wind, and vertical velocity. Our analyses have shown that vertical wind shear is significantly reduced over the northern SWIO during the El Niño years compared to the La Niña years (Figure 4(a)); however, it is largely enhanced in the southern part. Clearly, the reduced vertical wind shear is collocated with the enhanced DGPI in the north (Figure 3(c)), thus providing favorable environmental conditions for TC development. Accordingly, the vertical wind shear term is lower over the SWIO north of about 15˚S during El Niño years relative to La Niña years, which would favor a higher DGPI and thus higher TC genesis and frequency in the region.

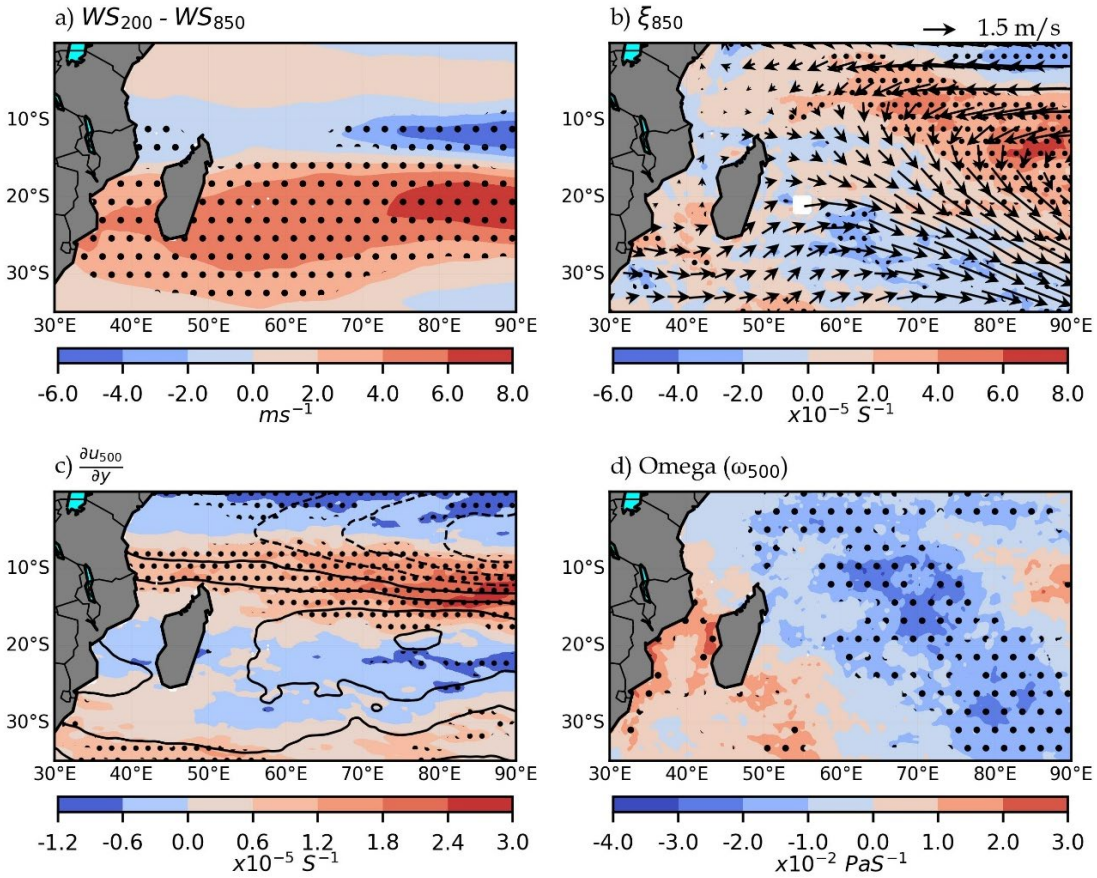

Figure 4. Differences of (a) vertical wind shear (WS_{200} - WS_{850}, m/s), (b) low-level vorticity (ξ_{850}, s^{-1}) and 850 hPa wind vectors, (c) meridional gradient of zonal wind ($-dU_{500}/dy$, s^{-1}) contours represents 500 hPa zonal wind (u), and (d) vertical velocity (ω_{500}, Pa/s) over the SWIO from November to April between El Niño and La Niña years during 1960-2022 from ERA5. The stippling indicates the difference is statistically significant at the 95% confidence level.

As shown in **Figure 4(b)**, a large part of the SWIO is dominated by large positive absolute vorticity anomalies, especially over the northeastern part of the SWIO and the Mozambique channel during the El Niño years relative to the La Niña years. Concurrently, there exits anomalous anticyclonic circulation at the low level in these SWIO regions. This implies that the low-level vorticity anomalies over the SWIO under the El Niño condition play a negative role, which is unfavorable for the spin and convergence required for TC genesis. Meanwhile, we also found some small negative absolute vorticity with cyclonic circulation anomaly in the southern part of the SWIO, which is conducive to initial spin and intensification of disturbances there. Overall, the change of low-level vorticity is not responsible for the increased DGPI and thus TC frequency over the SWIO during the El Niño years.

The meridional gradient of the zonal wind at 500 hPa is another important dynamic parameter in determining mid-level wind shear and resultant instabilities. During the El Niño years (**Figure 4(c)**), positive gradient anomalies are dominant over the SWIO north of about 15˚S, indicating a positive (i.e., anticyclonic) mid-

tropospheric vorticity anomaly that could suppress TC genesis potential over the northern SWIO. Meanwhile, there are small negative gradient anomalies in the south that would are favorable for convective organization and thus TC genesis there.

Figure 4(d) shows the difference of 500-hPa vertical pressure velocity over the SWIO between El Niño and La Niña years. Compared to La Niña years, there exits significant anomalous upward motions during El Niño years over most regions of the SWIO, which would favor enhanced convection activities and thus increased potential for tropical cyclone genesis. This spatial heterogeneity of vertical motion differences reveals how ENSO modulates the atmospheric dynamics over SWIO. For instance, the enhanced upward motion during El Niño years can be distinctly located over the eastern basin, collocating with the regions of frequent tropical cyclone genesis, while the anomalous subsidence during El Niño years is pronounced along the western margins, including the Mozambique channel, that would suppress convection activity and inhibit tropical cyclogenesis.

In summary, ENSO can modulate the DGPI and thus TC genesis and frequency over the SWIO mainly through altering vertical motion and vertical wind shear. Specifically, during El Niño years, enhanced upward motion and reduced vertical wind shear would favor tropical cyclogenesis mainly over the northern SWIO basin and also part of the east African coast, while stronger vorticity at both lower and middle levels and enhanced upward motion favor TC genesis development, particularly in the southeast part of the SWIO basin. These factors jointly increase DGPI over most areas of the SWIO basin and also shift the TC genesis region equatorward during El Niño years, although discrepancies with the actual TC frequency underline the role of mesoscale processes and variability. Our results are consistent with previous findings in Kuleshov et al. (2009) that there is a reduction of TC genesis in the western part of the South Indian Ocean basin and an increase in the east, as well as an equatorward displacement of the area favorable for TC genesis during El Niño events compared to La Niña events.

5. Interdecadal Variation of the ENSO-DGPI Relationship and the Role of IPO

The above results show that the SWIO DGPI is closely related to ENSO (with r = 0.5) during the period of 1960 to 2022. However, we further found that this interannual relationship varies over time. Figure 5 shows the 21-year moving correlation between the SWIO DGPI and the ENSO (blue line). Here, a higher (lower) positive correlation indicates that the SWIO DGPI is strongly (weakly) correlated with ENSO events. This means that the DGPI index tends to increase more (less) during El Niño years under high (low) correlation periods. Clearly, the correlation between the SWIO DGPI and ENSO relationship experiences notable interdecadal fluctuations, indicative of an unstable relationship between the two. Specifically, their interannual correlation is relatively high (with r above ~0.65) from the late 1970s to the early 1980s and during the early 1990s, while it is relatively low (with

r below ~0.45) during the early 1970s, the middle 1980s, and the early 2000s.

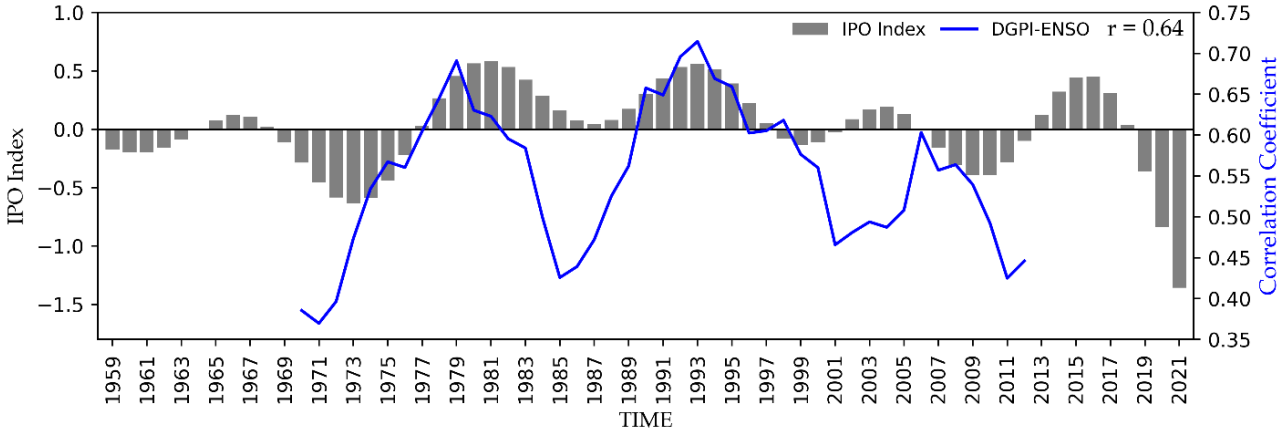

Figure 5. The 21-year moving correlation (blue line) between ENSO and DGPI over the SWIO, and the time series of the Interdecadal Pacific Oscillation (IPO) index (gray bars) during 1959-2022 based on ERA5. The correlation coefficient (r) between the two is given in the top-right corner.

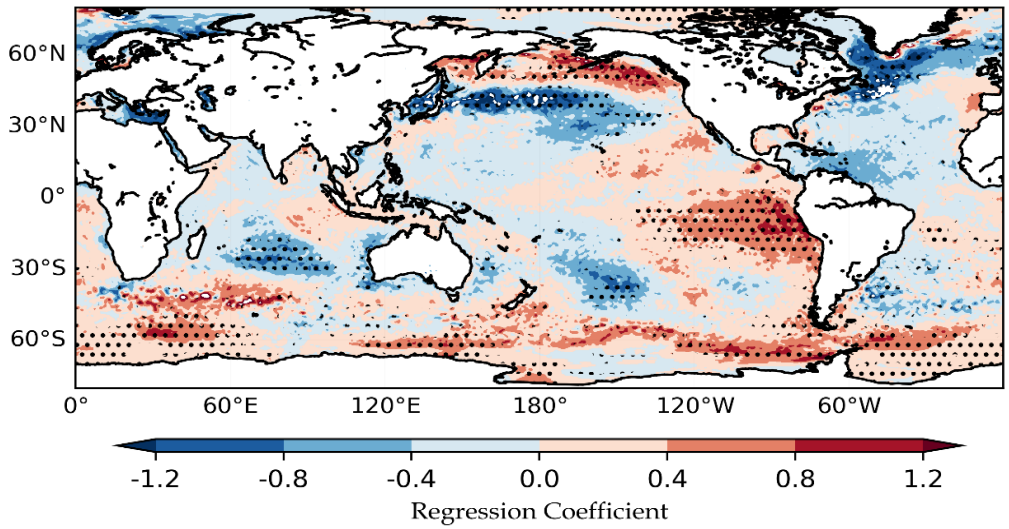

Figure 6. The regression map of the 21-year low-filtered SST anomalies onto the 21-year running correlation between ENSO and the SWIO DGPI (referring to the blue curve in **Figure 5**) from November to April during 1959 to 2022 based on ERA5. The stippling indicates the regression coefficient is statistically significant at the 95% confidence level.

Thus, one may wonder the reason why the interannual relationship between ENSO and the SWIO DGPI shows such interdecadal variations. Typically, the predominant interdecadal variations globally mainly come from low-frequency oceanic oscillations, including IPO and AMO. Given this, **Figure 6** shows the regression map of the DGPI-ENSO relationship and SST anomalies over the globe. It is found that there exists a significant positive relationship between the DGPI-ENSO relationship and SST anomalies over the eastern tropical Pacific. Conversely, a significant negative relationship occurs over the northern North Pacific (along ~45˚N) and southern Pacific. In addition, we also found a negative relationship

over the southeast of the Indian Ocean, this may suppress the TC genesis over this region. Overall, the SST regression pattern over the Pacific resembles the SST anomaly pattern associated with IPO, implying that IPO may play a role in modulating the relationship of the SWIO DGPI with ENSO events. To further confirm this point, we also show the IPO index in Figure 5 (gray bars). Clearly, the IPO index is positively correlated to the moving correlation between DGPI and ENSO, with a temporal correlation coefficient of 0.64, implying a close relationship between them. For instance, in the 1970's and early 1980's, the positive IPO phase similarly corresponds with stronger positive correlations between DGPI and ENSO. Conversely, in the late 1990s and early 2000s, which are characterized by negative IPO phases, there is a weaker and more variable correlation, with some years displaying near-neutral to negative correlations. In summary, these results indicate that the IPO likely modulates the interdecadal variation of the DGPI and ENSO relationship and thus TC genesis over the SWIO. This means that DGPI tends to be higher during El Niño years under positive IPO phases than under negative IPO phases.

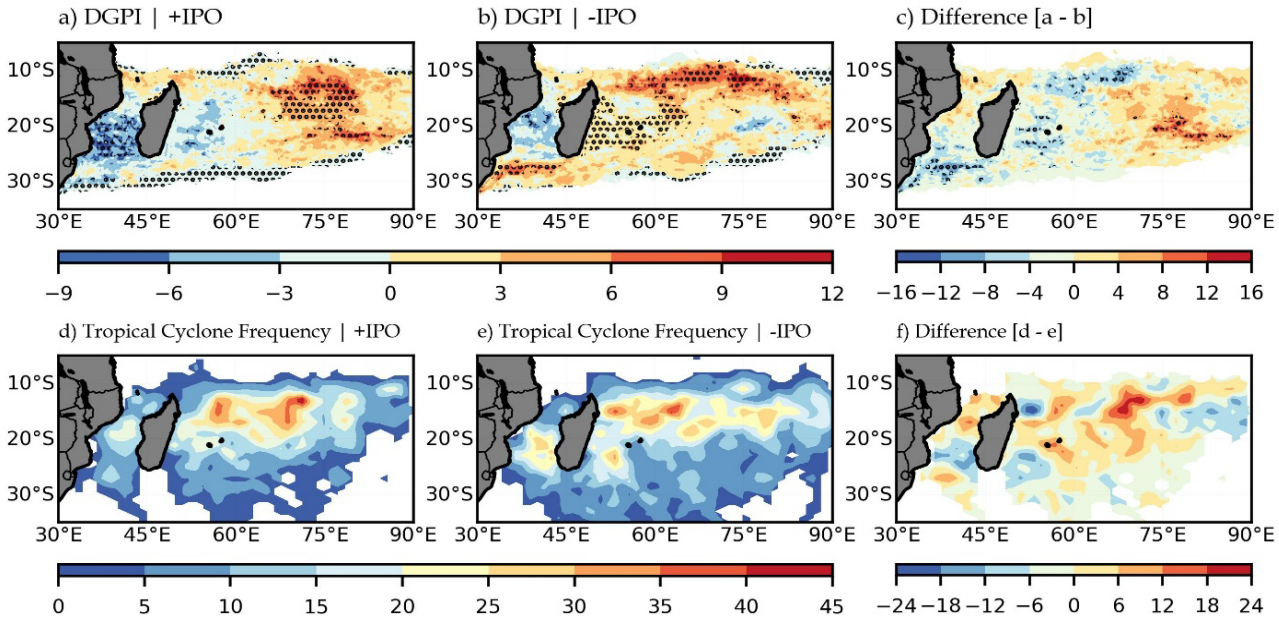

Figure 7. Spatial distribution of DGPI from November to April during (a) positive and (b) negative IPO phases and (c) their difference (i.e., positive phases minus negative phases) during 1959-2022 based on ERA5. (d)-(f) Same as (a)-(c), but for TC frequency based on IBTrACS. The stippling indicates the difference is statistically significant at the 95% confidence level.

To investigate the interdecadal variations of the ENSO-DGPI relationship and the role of IPO over the SWIO, we first analyze the composite of anomalous DGPI and TC frequency over the SWIO from November to April during positive and negative phases of IPO. Figure 7(a) reveals enhanced TC genesis potential in the central and northern coast of Mozambique. This increased DGPI corresponds with the increased TC frequency (Figure 7(d)) over the region during a positive IPO phase. In contrast, there is a noticeable reduction in TC genesis over central

but increased over the western SWIO (Figure 7(b)), consistent with the increased TC frequency over the Mozambique channel and the western SWIO (Figure 7(e)). As a result, the higher DGPI and TC frequency over the SWIO is observed during the positive IPO phase compared to the negative IPO phase (Figure 7(c), Figure 7(f)). Thus, the positive IPO phase acts to enhance both the TC genesis and the frequency of tropical cyclones over the central-eastern SWIO, which would thus favor more TCs during El Niño years. Conversely, the negative IPO phase appears to suppress both TC genesis and TC frequency there, leading to fewer TCs during El Niño years in this phase.

To further explore the role of IPO on the interdecadal variation of the ENSO-DGPI relationship over the SWIO, Figure 8 and Figure 9 compare several controlling factors related to TC genesis potential between El Niño and La Niña years under positive and negative IPO phases, respectively, including vertical wind shear, low-level vorticity, the meridional gradient of zonal wind, and vertical velocity. The above analyses have shown that vertical wind shear is significantly reduced over the northern SWIO during the El Niño years relative to the La Niña years for the whole selected period (Figure 4). This can also be seen under both IPO phases (Figure 8(a) and Figure 9(a)). However, the reduction of the vertical wind shear appears to be larger under the positive IPO phase (Figure 8(a)), compared to the negative IPO phase (Figure 9(a)), although it is largely enhanced in the central-to-southern SWIO. This largely reduced vertical wind shear is in accordance with the enhanced DGPI in the north during El Niño years under positive IPO phases (Figure 7(c)), thus providing favorable environmental conditions for TC development and TC frequency (Figure 7(e)).

As shown in Figure 8(b), significant positive absolute vorticity anomalies occur over the northwestern and southern SWIO during the El Niño years under positive IPO phases, while this anomalous anticyclonic vorticity is much stronger during the El Niño years under negative IPO phases (Figure 9(b)). This means that El Niño events would further decrease DGPI in this region when IPO is in its negative phases, which is not favorable for TC genesis. Furthermore, there also exits relatively strong negative absolute vorticity anomalies in the low level with cyclonic circulation anomaly in the central-eastern SWIO region during El Niño years under positive IPO phases (Figure 8(b)), whereas little vorticity anomalies occur there during El Niño years under negative IPO phases (Figure 9(b)). This implies that the low-level vorticity anomalies over the SWIO in the El Niño condition under positive IPO phases would be more favorable for the spin and convergence required for TC genesis, compared to that under negative IPO phases. Overall, the anomalous low-level vorticity condition related to ENSO events is more favorable for the interannual variability of DGPI over the SWIO (i.e., a high correlation between the two) under positive IPO phases, although the vorticity factor mainly acts to suppress TC genesis.

During the El Niño years, negative anomalies of 500-hPa zonal wind gradient are larger over the SWIO south of 15˚S under positive IPO phase (Figure 8(c))

than those under negative IPO phases (Figure 9(c)). This indicates a negative (i.e., cyclonic) mid-tropospheric vorticity anomaly that could enhance TC genesis potential over the southern SWIO during the El Niño years under positive IPO phases. Meanwhile, there are positive gradient anomalies in the north of 15˚S that would lead to a more stable atmosphere and reduced TC genesis there, but with a broader meridional range under negative IPO phases (Figure 9(c)) than under positive IPO phases (Figure 8(c)). This means that this factor would suppress TC genesis potential more and thus lead to a lower ENSO-DGPI correlation under negative IPO phases, relative to positive IPO phases.

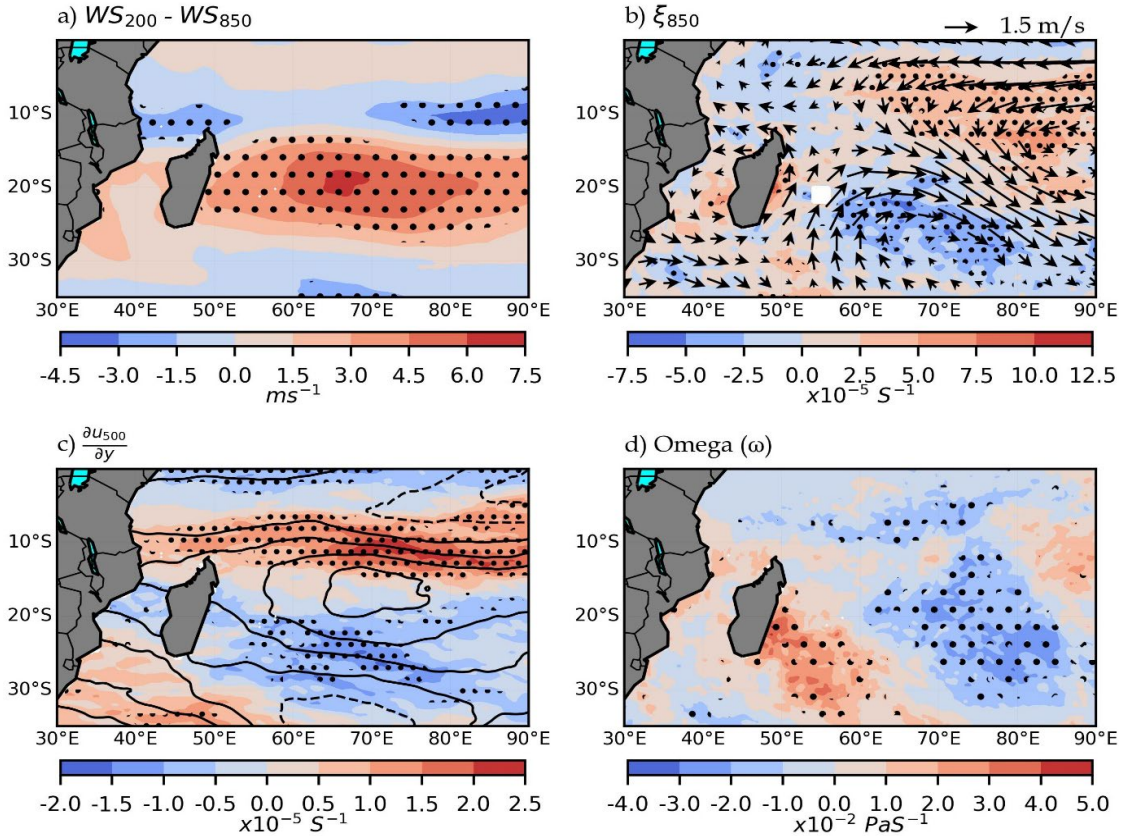

Figure 8. Differences of (a) vertical wind shear (WS_{200} - WS_{850}, m/s), (b) low-level vorticity (ξ_{850}, s^{-1}) and 850 hPa wind vectors, (c) meridional gradient of zonal wind ($-dU_{500}/dy$, s^{-1}) contours represents 500 hPa zonal wind (u), and (d) vertical velocity (ω_{500}, Pa/s) over the SWIO from November to April between El Niño and La Niña years under positive IPO phases during 1960-2022 from ERA5. The stippling indicates the difference is statistically significant at the 95% confidence level.

As shown in Figure 8(d), most areas of the SWIO are dominated by the significant anomalous upward motions over the central to southeastern part and some parts of the northern basin during the El Niño years under positive IPO phases. This condition would favor enhanced convection activities and thus increase the potential for tropical cyclone genesis over the area. Meanwhile, during the El Niño years under the negative IPO phases (Figure 9(d)), the significant anomalous upward motions shift northward of the SWIO and to the northeast coast of Mada-

gascar island. This can be supported by Figure 7(b) in that there is higher DGPI and TC occurrence frequency over the northern part of SWIO under negative IPO phases. Besides, the anomalous subsidence in the Mozambique channel during the El Niño years under the negative IPO phase would suppress the conducive environment for convective activities and inhibit tropical cyclogenesis over the area.

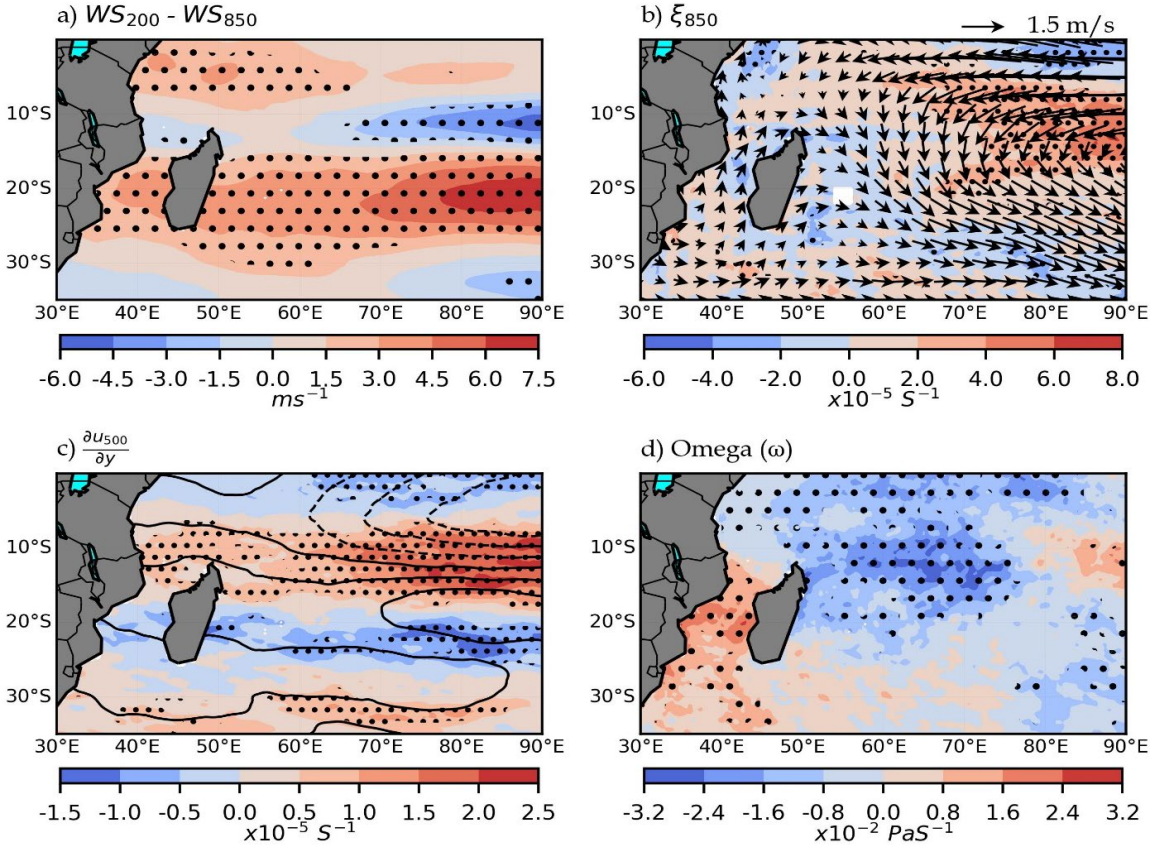

Figure 9. Same as Figure 8, but under negative IPO phases.

In summary, the IPO was found to play a critical role in shaping environmental factors that influence TC genesis and frequency over the SWIO and their relationship with ENSO. From the above analysis, it has been found that during El Niño years under positive IPO phases, reduced vertical wind shear in the northern SWIO creates favorable conditions for TC formation, while enhanced wind shear in the central of the SWIO presents mixed effects. Low-level vorticity decreases with enhanced anomalous cyclonic circulation in positive IPO phases, which would lead to TC genesis formation over the area, while the absolute vorticity is further increased with enhanced anomalous anticyclonic circulation in negative IPO phases that suppresses TC development and its relation with ENSO. The 500-hPa meridional gradient of zonal wind shows larger negative anomalies in the southern SWIO during El Niño years under positive IPO phases, thus favoring enhanced TC genesis and its relation with ENSO. Vertical velocity patterns indicate anomalous upward motion in the eastern SWIO during positive IPO phases,

supporting stronger convection and TC development. As a result, both ENSO-related anomalies of these controlling factors are more favorable for TC genesis and occurrence under positive IPO phases than negative IPO phases, which ultimately promotes higher ENSO-DGPI correlations.

6. Conclusion

In this study, we investigate the interannual relationship between ENSO and TC genesis potential over the Southwest Indian Ocean (SWIO) from November to April based on the Dynamic Genesis Potential Index (DGPI) and further explore the modulation of this relationship by the Interdecadal Pacific Oscillation (IPO) using ERA5 reanalysis during 1959-2022. The main results are as follows:

1) The DGPI can effectively portray TC genesis potential over the SWIO, with strong spatial and temporal correlations with observed TC activity. A distinct seasonality in DGPI aligns with the peak TC season (November-April), highlighting its utility as a proxy for tropical cyclogenesis.

2) The TC genesis (as measured by DGPI) is positively correlated with ENSO events, implying a crucial role of ENSO in impacting TC genesis over the SWIO. Specifically, the DGPI increases (decreases) remarkably with enhanced (suppressed) TC genesis and higher (lower) TC frequency over the SWIO during El Niño (La Niño) years. This interannual relationship is primarily contributed by reduced vertical wind shear and enhanced upward motion in the SWIO during El Niño years.

3) The interannual ENSO-DGPI relationship exhibits notable interdecadal variations, which is closely related to IPO; that is, their interannual correlation is relatively strong (weak) under positive (negative) IPO phases. Compared to the negative IPO phases, the positive IPO phase favors TC genesis over the SWIO through reinforcing ENSO-driven reduction in vertical wind shear and anomalous upward motion, together with low-level cyclonic vorticity over the central SWIO.

Overall, our results suggest that ENSO and IPO are both decisive factors in portraying the TC genesis potential over the SWIO. The findings contribute to a deeper understanding of the interannual and interdecadal variability of TC activity in the region, offering valuable insights for improving seasonal forecasting and long-term TC risk assessment.

Conflicts of Interest

The authors declare no conflicts of interest regarding the publication of this paper.

References

Bister, M., & Emanuel, K. A. (2002). Low Frequency Variability of Tropical Cyclone Potential Intensity 1. Interannual to Interdecadal Variability. *Journal of Geophysical Research: Atmospheres, 107,* ACL 26-1-ACL 26-15. https://doi.org/10.1029/2001jd000776

Camargo, S. J., & Wing, A. A. (2016). Tropical Cyclones in Climate Models. *WIREs Climate Change, 7,* 211-237. https://doi.org/10.1002/wcc.373

Camargo, S. J., Emanuel, K. A., & Sobel, A. H. (2007). Use of a Genesis Potential Index to

Diagnose ENSO Effects on Tropical Cyclone Genesis. *Journal of Climate, 20,* 4819-4834. https://doi.org/10.1175/jcli4282.1

Crowley, T. J., Obrochta, S. P., & Liu, J. (2014). Recent Global Temperature "Plateau" in the Context of a New Proxy Reconstruction. *Earth's Future, 2,* 281-294. https://doi.org/10.1002/2013ef000216

Duan, W., Yuan, J., Duan, X., & Feng, D. (2021). Seasonal Variation of Tropical Cyclone Genesis and the Related Large-Scale Environments: Comparison between the Bay of Bengal and Arabian Sea Sub-Basins. *Atmosphere, 12,* Article No. 1593. https://doi.org/10.3390/atmos12121593

England, M. H., McGregor, S., Spence, P., Meehl, G. A., Timmermann, A., Cai, W. et al. (2014). Recent Intensification of Wind-Driven Circulation in the Pacific and the Ongoing Warming Hiatus. *Nature Climate Change, 4,* 222-227. https://doi.org/10.1038/nclimate2106

Fyfe, J. C., Meehl, G. A., England, M. H., Mann, M. E., Santer, B. D., Flato, G. M. et al. (2016). Making Sense of the Early-2000s Warming Slowdown. *Nature Climate Change, 6,* 224-228. https://doi.org/10.1038/nclimate2938

Gershunov, A., & Barnett, T. P. (1998). Interdecadal Modulation of ENSO Teleconnections. *Bulletin of the American Meteorological Society, 79,* 2715-2725. https://doi.org/10.1175/1520-0477(1998)079<2715:imoet>2.0.co;2

Gray, W. M. (1979). Hurricanes: Their Formation, Structure and Likely Role in the Tropical Circulation. In D. B. Shaw (Ed.), *Supplement to Meteorology over the Tropical Oceans* (pp. 155-218). James Glaisher House.

Henley, B. J. (2017). Pacific Decadal Climate Variability: Indices, Patterns and Tropical-Extratropical Interactions. *Global and Planetary Change, 155,* 42-55. https://doi.org/10.1016/j.gloplacha.2017.06.004

Henley, B. J., Gergis, J., Karoly, D. J., Power, S., Kennedy, J., & Folland, C. K. (2015). A Tripole Index for the Interdecadal Pacific Oscillation. *Climate Dynamics, 45,* 3077-3090. https://doi.org/10.1007/s00382-015-2525-1

Hersbach, H., Bell, B., Berrisford, P., Biavati, G., Horányi, A., Muñoz Sabater, J., Nicolas, J., Peubey, C., Radu, R., Rozum, I., Schepers, D., Simmons, A., Soci, C., Dee, D., & Thépaut, J.-N. (2023). *ERA5 Monthly Averaged Data on Single Levels from 1940 to Present*. Copernicus Climate Change Service (C3S) Climate Data Store (CDS). https://doi.org/10.24381/cds.f17050d7

Ho, C., Kim, J., Jeong, J., Kim, H., & Chen, D. (2006). Variation of Tropical Cyclone Activity in the South Indian Ocean: El Niño-Southern Oscillation and Madden-Julian Oscillation Effects. *Journal of Geophysical Research: Atmospheres, 111.* https://doi.org/10.1029/2006JD007289

Hsieh, T., Zhang, B., Yang, W., Vecchi, G. A., Zhao, M., Soden, B. J. et al. (2023). The Influence of Large-Scale Radiation Anomalies on Tropical Cyclone Frequency. *Journal of Climate, 36,* 5431-5441. https://doi.org/10.1175/jcli-d-22-0449.1

Knapp, K. R., Kruk, M. C., Levinson, D. H., Diamond, H. J., & Neumann, C. J. (2010). The International Best Track Archive for Climate Stewardship (IBTrACS). *Bulletin of the American Meteorological Society, 91,* 363-376. https://doi.org/10.1175/2009bams2755.1

Kosaka, Y., & Xie, S. (2013). Recent Global-Warming Hiatus Tied to Equatorial Pacific Surface Cooling. *Nature, 501,* 403-407. https://doi.org/10.1038/nature12534

Kosaka, Y., & Xie, S. (2016). The Tropical Pacific as a Key Pacemaker of the Variable Rates of Global Warming. *Nature Geoscience, 9,* 669-673. https://doi.org/10.1038/ngeo2770

Kuleshov, Y., Chane Ming, F., Qi, L., Chouaibou, I., Hoareau, C., & Roux, F. (2009). Trop-

ical Cyclone Genesis in the Southern Hemisphere and Its Relationship with the ENSO. *Annales Geophysicae, 27,* 2523-2538. https://doi.org/10.5194/angeo-27-2523-2009

Li, W., Li, L., & Deng, Y. (2015). Impact of the Interdecadal Pacific Oscillation on Tropical Cyclone Activity in the North Atlantic and Eastern North Pacific. *Scientific Reports, 5,* Article No. 12358. https://doi.org/10.1038/srep12358

Livezey, R. E., & Smith, T. M. (1999). Covariability of Aspects of North American Climate with Global Sea Surface Temperatures on Interannual to Interdecadal Timescales. *Journal of Climate, 12,* 289-302. https://doi.org/10.1175/1520-0442-12.1.289

Lorenzo, E. Di, Xu, T., Zhao, Y., Newman, M., Capotondi, A., Stevenson, S., Amaya, D. J., Anderson, B. T., Ding, R., Furtado, J. C., Joh, Y., Liguori, G., Lou, J., Miller, A. J., Navarra, G., Schneider, N., Vimont, D. J., Wu, S., & Zhang, H. (2025). Modes and Mechanisms of Pacific Decadal-Scale Variability. *Annual Review of Marine Science, 15,* 249-275.

Maher, N., Gupta, A. S., & England, M. H. (2014). Drivers of Decadal Hiatus Periods in the 20th and 21st Centuries. *Geophysical Research Letters, 41,* 5978-5986. https://doi.org/10.1002/2014gl060527

Mavume, A., Rydberg, L., Rouault, M., & Lutjeharms, J. (2010). Climatology and Landfall of Tropical Cyclones in the South-West Indian Ocean. *Western Indian Ocean Journal of Marine Science, 8,* 15-36. https://doi.org/10.4314/wiojms.v8i1.56672

Moore, G. W. K., Halfar, J., Majeed, H., Adey, W., & Kronz, A. (2017). Amplification of the Atlantic Multidecadal Oscillation Associated with the Onset of the Industrial-Era Warming. *Scientific Reports, 7,* Article No. 40861. https://doi.org/10.1038/srep40861

Murakami, H., & Wang, B. (2022). Patterns and Frequency of Projected Future Tropical Cyclone Genesis Are Governed by Dynamic Effects. *Communications Earth & Environment, 3,* Article No. 77. https://doi.org/10.1038/s43247-022-00410-z

Muthige, M. S., Malherbe, J., Englebrecht, F. A., Grab, S., Beraki, A., Maisha, T. R. et al. (2018). Projected Changes in Tropical Cyclones over the South-West Indian Ocean under Different Extents of Global Warming. *Environmental Research Letters, 13,* Article ID: 065019. https://doi.org/10.1088/1748-9326/aabc60

Power, S., Casey, T., Folland, C., Colman, A., & Mehta, V. (1999). Inter-Decadal Modulation of the Impact of ENSO on Australia. *Climate Dynamics, 15,* 319-324. https://doi.org/10.1007/s003820050284

Wang, B., & Chan, J. C. L. (2002). How Strong ENSO Events Affect Tropical Storm Activity over the Western North Pacific. *Journal of Climate, 15,* 1643-1658. https://doi.org/10.1175/1520-0442(2002)015<1643:hseeat>2.0.co;2

Wang, B., & Murakami, H. (2020). Dynamic Genesis Potential Index for Diagnosing Present-Day and Future Global Tropical Cyclone Genesis. *Environmental Research Letters, 15,* Article ID: 114008. https://doi.org/10.1088/1748-9326/abbb01